PROCEEDINGS OF SCIENCE

Revisiting a light NMSSM pseudoscalar at the LHC

Nils-Erik Bomark,[a] **Stefano Moretti,**[b] **Shoaib Munir**[*c] **and Leszek Roszkowski**[a]

[a]*National Centre for Nuclear Research*
Hoża 69, 00-681 Warsaw, Poland
[b]*School of Physics & Astronomy, University of Southampton*
Southampton SO17 1BJ, UK
[c]*Department of Physics and Astronomy, Uppsala University*
Box 516, SE-751 20 Uppsala, Sweden
E-mail: nbomark@fuw.edu.pl, s.moretti@soton.ac.uk, shoaib.munir@physics.uu.se, leszek.roszkowski@fuw.edu.pl

The discovery of a light, singlet-like pseudoscalar Higgs boson, A_1, of the Next-to-Minimal Supersymmetric Standard Model (NMSSM) could provide a hallmark signature of non-minimal supersymmetry. We review here the potential of the LHC to probe such a light A_1 in the decays of one of the heavier scalar Higgs bosons of the NMSSM. We find the production of pairs of the A_1, with a mass below 60 GeV or so, via decays of the two lightest scalar states to be especially promising, for an integrated luminosity as low as 30/fb. For heavier masses, the decay of the heaviest scalar into a Z boson and an A_1 could lead to its detection at the LHC.

Prospects for Charged Higgs Discovery at Colliders - CHARGED 2014,
16-18 September 2014
Uppsala University, Sweden

*Speaker.

© Copyright owned by the author(s) under the terms of the Creative Commons Attribution-NonCommercial-ShareAlike Licence.

PoS(Charged2014)029

1. Introduction

The NMSSM contains an extra singlet Higgs superfield in addition to the two doublet superfields of the Minimal Supersymmetric Standard Model. As a result, there are a total of five neutral Higgs mass eigenstates: scalars H_i, with $i = 1,2,3$, and pseudoscalars $A_{1,2}$, and a charged pair $H^{\pm}$, in the model. The masses of the two new singlet-like states are generally very weakly constrained by the Higgs boson data from the Large Electron Positron collider or the Large Hadron Collider (LHC), and can be as low as a few GeV. We assess the scope of the detectability of a light, $\lesssim 150\,\text{GeV}$, A_1 of the NMSSM at the run 2 of the LHC with $\sqrt{s} = 14\,\text{TeV}$. Through dedicated scans of the parameter space of the contrained NMSSM with non-universal Higgs masses (CNMSSM-NUHM), we found a considerable number of points containing such A_1 while also satisfying important experimental constraints. We then performed a detailed signal-to-background analysis for each of the main production and decay channels of A_1. Most notably, we employed the jet substructure method for detecting the b-quarks originating from A_1 decays, which considerably improves the experimental sensitvitiy.

2. A_1 production channels in the model studied

The soft supersymmetry (SUSY)-breaking Higgs potential of the NMSSM is written as

$$V_{\text{soft}} = m_{H_u}^2 |H_u|^2 + m_{H_d}^2 |H_d|^2 + m_S^2 |S|^2 + \left(\lambda A_\lambda S H_u H_d + \frac{1}{3} \kappa A_\kappa S^3 + \text{h.c.} \right), \tag{2.1}$$

where λ and κ are dimensionless couplings and A_λ and A_κ are trilinear soft parameters. In the CNMSSM-NUHM the soft masses of the Higgs fields m_{H_u}, m_{H_d} and m_S are separated from the unified scalar mass parameter m_0 at the grand unification (GUT) scale. These three masses can be traded at the electroweak (EW) scale for the parameters $\tan\beta$ ($\equiv v_u/v_d$, with v_u being the vacuum expectation value (VEV) of the u-type Higgs doublet and v_d that of the d-type one), μ_{eff} ($\equiv \lambda\, s$, with s being the VEV of the singlet field) and κ. Similarly $A_\lambda{}^*$ and $A_\kappa{}^*$ (with the * implying that these are defined at the GUT scale) are also disunified from the trilinear coupling parameter A_0. The CNMSSM-NUHM thus contains a total of nine continuous input parameters, which are given in table 1 along with their ranges scanned for this study. These ranges correspond to the 'naturalness limit' of the model, where H_2 with a mass consistent with that of the Higgs boson discovered at the LHC [2, 3] can be obtained without requiring large radiative corrections from the stop sector.

The tree-level mass-squared of the A_1 in the NMSSM is written in terms of the above parameters (defined at the SUSY-breaking scale), assuming negligible singlet-doublet mixing, as

$$m_{A_1}^2 \simeq \frac{A_\lambda}{2s} v^2 \lambda \sin 2\beta + \kappa (2v^2 \lambda \sin 2\beta - 3sA_\kappa), \tag{2.2}$$

where $v \equiv \sqrt{v_u^2 + v_d^2} \simeq 174\,\text{GeV}$. At the LHC, the A_1 can either be produced directly, preferably in the $gg \to bbA_1$ channel, owing to the possibility of a considerably enhanced $b\bar{b}A_1$ coupling [1] compared to the ggA_1 effective coupling. Alternatively, each of H_i, produced in the gluon-fusion (GF) mode, can also decay into A_1A_1 or A_1Z pairs, when kinematically allowed. Here we will consider only these indirect production modes.

PoS(Charged2014)029

Parameter	m_0 (GeV)	$m_{1/2}$ (GeV)	A_0 (GeV)	$\mu_{\rm eff}$ (GeV)
Range	200 – 2000	100 – 1000	−3000 – 0	100 – 200
$\tan\beta$	λ	κ	$A_\lambda{}^*$ (GeV)	$A_\kappa{}^*$ (GeV)
1 – 6	0.4 – 0.7	0.01 – 0.7	−500 – 500	−500 – 500

Table 1: The CNMSSM-NUHM input parameters and their scanned ranges.

In particular, in case of the decaying SM-like H_2, the mass measurement of $\sim 125\,$GeV serves as an important kinematical handle. Removing this condition (for H_1 and H_3) reduces the sensitivity by a factor of 2 to 3. The A_1A_1 pair thus produced decays via the $b\bar{b}b\bar{b}$ ($4b$), $b\bar{b}\tau^+\tau^-$ ($2b2\tau$) and $\tau^+\tau^-\tau^+\tau^-$ (4τ) final state combinations. In the case of A_1Z production, we only take the $Z\to\ell^+\ell^-$ decay into account, where $\ell^+\ell^-$ (2ℓ) stands for $\mu^+\mu^-$ and e^+e^- combined.

3. Parameter scans and event analysis

We scanned the NMSSM parameter space, given in table 1, to search for regions yielding $m_{A_1} \lesssim 150\,$GeV and the mass of H_2, m_{H_2}, around 125 GeV. We used the publicly available package NMSSMTools-v4.2.1 [4] for computation of the SUSY mass spectrum and branching ratios (BR) of the Higgs bosons for each model point. In our scans we imposed the constraints from b-physics, based on [6], and from Dark Matter relic density measurement [7], as

- $\mathrm{BR}\,(\mathrm{B_s}\to\mu^+\mu^-) = (3.2\ (\pm 10\%\ \text{theoetical error}) \pm 1.35)\times 10^{-9}$,
- $\mathrm{BR}\,(\mathrm{B_u}\to\tau\nu) = (1.66\pm 0.66\pm 0.38)\times 10^{-4}$,
- $\mathrm{BR}\,(\overline{\mathrm{B}}\to \mathrm{X_s}\gamma) = (3.43\pm 0.22\pm 0.21)\times 10^{-4}$,
- $\Omega_\chi h^2 < 0.131\ (0.119 + 10\%\ \text{theoetical error})$.

Exclusion limits from the LEP and LHC Higgs boson searches were also tested against using the HiggsBounds-v4.1.3 [8] package. Finally, from NMSSMTools we obtained the signal rates of H_2, defined for a given decay channel X as

$$R_X \equiv \frac{\sigma(gg\to H_2)\times \mathrm{BR}(H_i\to X)}{\sigma(gg\to h_{\rm SM})\times \mathrm{BR}(h_{\rm SM}\to X)}\,, \tag{3.1}$$

where $h_{\rm SM}$ is the SM Higgs boson with the same mass as H_2. We then required R_X for $X=\gamma\gamma, ZZ$ to lie within the measured $\pm 1\sigma$ ranges of the corresponding experimental quantities μ_X by the CMS collaboration [5]. These ranges read

$$\mu_{\gamma\gamma} = 1.13\pm 0.24 \quad\text{and}\quad \mu_{ZZ} = 1.0\pm 0.29\,. \tag{3.2}$$

Following the scans, we carried out a dedicated signal-to-background analysis based on Monte Carlo event generation for proton-proton collisions at 14 TeV centre-of-mass energy at the LHC, for each process of interest. Using the program SuSHi-v1.1.1 [9], we first calculated the GF production cross section of an SM Higgs boson with the same mass as as that of a H_i which is expected to decay

PoS(Charged2014)029

into A_1A_1 or A_1Z for a given SUSY point. This cross section was then rescaled using the ggH_i reduced coupling in the NMSSM, and multiplied by the relevant BRs of the H_i, all of which are obtained from NMSSMTools. The backgrounds, which include the $pp \to 4b$, $pp \to 2b2\tau$, $pp \to 4\tau$, $pp \to Z2b$ and $pp \to Z2\tau$ processes, were computed with MadGraph 5 [12]. Both the signal and the background for each process were hadronised and fragmented using Pythia 8.180 [10] interfaced with FastJet-v3.0.6 [11] for jet clustering. The parton-level acceptance cuts used are

- $|\eta| < 2.5$ for all final state objects,
- $p_T > 15\,\text{GeV}$ far all final state objects,
- $\Delta R \equiv \sqrt{(\Delta\eta)^2 + (\Delta\phi)^2} > 0.2$ for all b-quark pairs,
- $\Delta R > 0.4$ for all other pairs of final state objects,

where p_T, η, ϕ are the transverse momentum, pseudorapidity and azimuthal angle, respectively.

Our use of the jet substructure method [13] implied that we had three possible signatures for a decaying A_1: one fat jet, two single b-jets and two τ-jets. The fat jet analysis, which assumes boosted b-quarks, allows one to obtain much higher sensitivities, particularly for large masses of the decaying Higgs bosons. We then calculated the expected cross sections for the signal processes which yield $S/\sqrt{B} > 5$ for three benchmark accumulated luminosities at the LHC, $\mathscr{L} = 30/\text{fb}, 300/\text{fb}$ and $3000/\text{fb}$, in various final state combinations, as functions of m_{A_1}.

4. Results

For the figures shown in this section, we first make two assertions: 1) all the points shown satisfy the constraints mentioned earlier and yield $122\,\text{GeV} < m_{H_2} < 129\,\text{GeV}$, and 2) the sensitivity curve(s) shown corresponds to the best final state combination(s) for probing the given process.

Production via $H_2 \to A_1A_1/Z$: We begin with the decays of the SM-like H_2, since reconstructing its correct mass improves the kinematics, as noted earlier. In figure 1(a) we show the prospects for the $H_2 \to A_1A_1$ channel at the LHC. Also shown are the sensitivity curves for the $2b2\tau$ final state at $\mathscr{L} = 30/\text{fb}$ and for the 4τ final state at $\mathscr{L} = 3000/\text{fb}$. We see that a large part of the NMSSM parameter space can be probed via $H_2 \to A_1A_1$ decays at the LHC, at $\mathscr{L}$ as low as 30/fb. Note that the Higgs boson signal rate constraints from CMS restrict the BR($H_2 \to A_1A_1$) to less than 50%. In figure 1(b) we see that the $H_2 \to A_1Z$ decay shows no promise even at $\mathscr{L} = 3000/\text{fb}$.

Production via $H_{1,3} \to A_1A_1/Z$: The case of the $H_1 \to A_1A_1$ decay, for a singlet-like H_1, is illustrated in figure 2(a). One sees that almost all the points with $m_A \gtrsim 12\,\text{GeV}$ are potentially discoverable in the $2b2\tau$ final state at $\mathscr{L} = 30/\text{fb}$. Two separate sensitivity curves corresponding to this final state indicate that for low A_1 masses the fat jet analysis has been employed, which results in a better reach. Even lighter A_1 could also be visible in the 4τ final state with $\mathscr{L} = 300/\text{fb}$. Figure 2(b) shows poor prospects for the discovery of A_1 via the $H_1 \to A_1Z$ channel also.

In figure 3(a) we see that the $H_3 \to A_1A_1$ channel will be inaccessible at the LHC due to the fact that for such high masses of H_3 ($\gtrsim 400\,\text{GeV}$) the production cross section gets diminished.

PoS(Charged2014)029

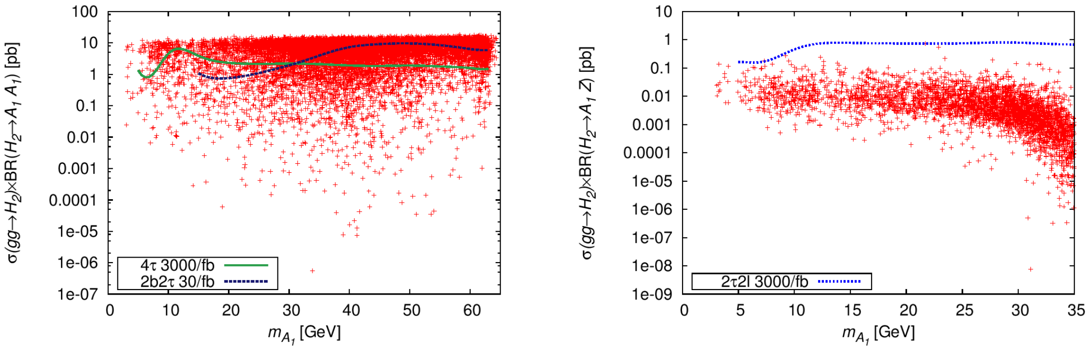

(a) (b)

Figure 1: Cross sections for (a) the $gg \to H_2 \to A_1A_1$ process and (b) the $gg \to H_2 \to A_1Z$ process.

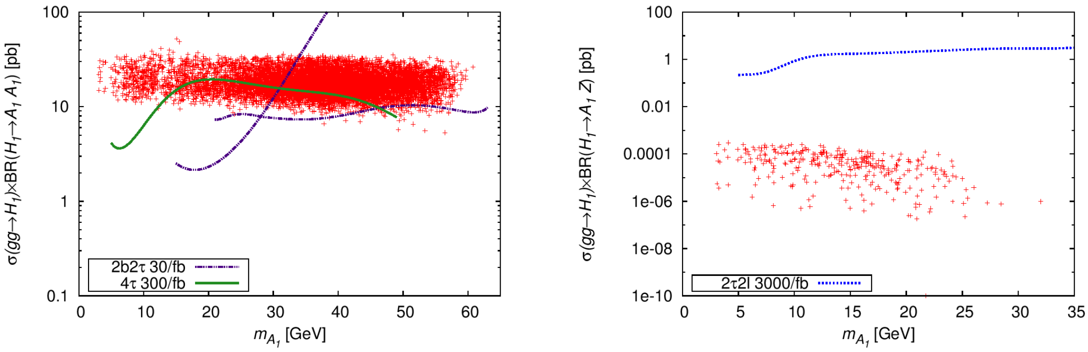

(a) (b)

Figure 2: Cross sections for (a) the $gg \to H_1 \to A_1A_1$ process and (b) the $gg \to H_1 \to A_1Z$ process.

Moreover, other decay channels of H_3 dominate over this channel. The sensitivity curve in the figure corresponds to the $2b2\tau$ final state for $\mathscr{L} = 3000$/fb. Conversely, as shown in figure 3(b), in the $H_3 \to A_1Z$ channel a number of points lie above the $2b2\ell$ sensitivity curve for $\mathscr{L} = 300$/fb. The discoverability of an A_1 in this channel results from the use of the fat jet analysis as well as from a sizeable H_3A_1Z coupling, owing to a significant doublet component in A_1.

In summary, the decays of the two lightest scalar Higgs bosons carry the potential to reveal an A_1 with mass $\lesssim 60$ GeV for an integrated luminosity of 30/fb at the LHC. When the A_1 is heavier than ~ 60 GeV, while its pair production also becomes inaccessible, the $gg \to H_3 \to A_1Z$ channel takes over as the most promising one. This channel is, therefore, of great importance and warrants dedicated probes in future analyses at the LHC.

Acknowledgments

This work has been funded in part by the Welcome Programme of the Foundation for Polish Science. S. Moretti is supported in part through the NExT Institute. S. Munir is supported in part by the Swedish Research Council under contracts 2007-4071 and 621-2011-5107. The use of the CIS computer cluster at NCBJ is gratefully acknowledged.

PoS(Charged2014)029

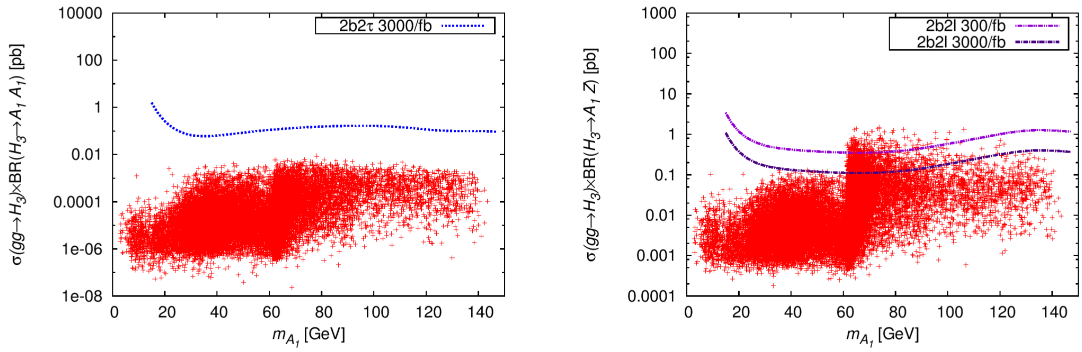

(a) (b)

Figure 3: Cross sections for (a) the $gg \to H_3 \to A_1A_1$ process and (b) the $gg \to H_3 \to A_1Z$ process.

References

[1] S. Munir, L. Roszkowski and S. Trojanowski, *Simultaneous enhancement in $\gamma\gamma$, $b\bar{b}$ and $\tau^+\tau^-$ rates in the NMSSM with nearly degenerate scalar and pseudoscalar Higgs bosons*, *Phys. Rev.* **D88** (2013) 055017 [arXiv:1305.0591].

[2] S. Chatrchyan et al. (CMS Collaboration), *Observation of a new boson at a mass of 125 GeV with the CMS experiment at the LHC*, *Phys. Lett.* **B716** (2012) 30–61 [arXiv:1207.7235].

[3] G. Aad et al. (ATLAS Collaboration), *Observation of a new particle in the search for the Standard Model Higgs boson with the ATLAS detector at the LHC*, *Phys. Lett.* **B716** (2012) 1–29 [arXiv:1207.7214].

[4] www.th.u-psud.fr/NMHDECAY/nmssmtools.html.

[5] CMS Collaboration, *Precise determination of the mass of the Higgs boson and studies of the compatibility of its couplings with the standard model*, **CMS PAS HIG-14-009** (2014).

[6] J. Beringer et al. (PDG Collaboration), *Review of Particle Physics*, *Phys. Rev.* **D86** (2012) 010001.

[7] P. A. R. Ade et al. (Planck Collaboration), *Planck 2013 results. XVI. Cosmological parameters*, *Astron. Astrophys.* **571** (2014) A16 [arXiv:1303.5076].

[8] P. Bechtle et al., *HiggsBounds-4: Improved Tests of Extended Higgs Sectors against Exclusion Bounds from LEP, the Tevatron and the LHC*, *Eur. Phys. J.* **C74** (2014) 2693 [arXiv:1311.0055].

[9] R. V. Harlander, S. Liebler and H. Mantler, *SusHi: A program for the calculation of Higgs production in gluon fusion and bottom-quark annihilation in the Standard Model and the MSSM*, *Comput. Phys. Commun.* **184** (2013) 1605–1617 [arXiv:1212.3249].

[10] T. Sjostrand, S. Mrenna and P. Z. Skands, *A Brief Introduction to PYTHIA 8.1*, *Comput. Phys. Commun.* **178** (2008) 852–867 [arXiv:0710.3820].

[11] M. Cacciari, G. P. Salam and G. Soyez, *FastJet User Manual*, *Eur. Phys. J.* **C72** (2012) 1896 [arXiv:1111.6097].

[12] J. Alwall et al., *MadGraph 5: Going Beyond*,*JHEP* **1106** (2011) 128 [arXiv:1106.0522].

[13] J. M. Butterworth, A. R. Davison, M. Rubin and G. P. Salam, *Jet substructure as a new Higgs search channel at the LHC*, *Phys. Rev. Lett.* **100** (2008) 242001 [arXiv:0802.2470].

PoS(Charged2014)029